GEOLOGICA CARPATHICA, DECEMBER 2012, 63, 6, 503–512 doi: 10.2478/v10096-012-0039-x

Stability of kaolin sand from the Vyšný Petrovec deposit (south Slovakia) in an acid environment

MARTIN PENTRÁK[1]✉, JANA MADEJOVÁ[1], SLÁVKA ANDREJKOVIČOVÁ[1], PETER UHLÍK[2] and PETER KOMADEL[1]

[1]Institute of Inorganic Chemistry, Slovak Academy of Sciences, SK-845 36 Bratislava, Slovak Republic; ✉martin.pentrak@savba.sk
[2]Department of Geology of Mineral Deposits, Comenius University, Mlynská dolina G, SK-842 15 Bratislava, Slovak Republic

(Manuscript received October 27, 2011; accepted in revised form June 13, 2012)

Abstract: Comprehensive characterization of kaolin sand from the Vyšný Petrovec (VP) deposit in Slovakia by a variety of experimental methods was performed. The quantitative XRD analysis (RockJock software) revealed that the acid-untreated sample contained mainly kaolinite (~60 wt. %), a considerable amount of dioctahedral micas (~32 wt. %) and quartz (~7 wt. %). The Hinckley index (HI) and Aparicio-Galán-Ferrel index (AGFI) calculated from the *02l* and *11l* reflections showed medium-defect kaolinite to be present in the VP kaolin. The influence of the mineral composition of VP kaolin on its stability in 6 mol·dm^{-3} HCl at 95 °C was investigated. The solid reaction products were examined by chemical analysis; XRD and infrared spectroscopy in both middle (MIR) and near (NIR) regions. Considerably higher dissolution rate of Fe compared to Al indicated that Fe was bounded in a readily soluble phase rather than in kaolinite. While the MIR spectra confirmed the gradual release of the central atoms from the clay minerals layers and creation of amorphous silica upon acid treatment, the NIR spectra revealed the formation of Si-OH groups in the solid reaction product. Relatively high dissolution rate of VP kaolin resulted from the presence of small-grains of medium-defect kaolinite and clay admixtures in VP kaolin sand.

Key words: acid treatment, thermal analysis, SEM, XRD analysis, FTIR spectroscopy, kaolinite.

Introduction

Kaolins are raw materials extensively used in a wide variety of industrial applications. The main constituent of kaolins is the clay mineral kaolinite with specific properties and structure determining its use for technological utilization of whole kaolin ore (He et al. 2011; Ma 2011; Moussi et al. 2011; Yanik 2011), for example, in ceramic production, as fillers for plastics and rubber (Lagaly 1999), but the largest amounts of processed kaolins, more than 60 % of the word production, are used in the paper industry as fillers within the network of cellulose fibres and as coating particles (Harvey & Lagaly 2006; Murray 2007). The next utilization of kaolinite is in preparation of nanotubes (Matusik et al. 2009, 2011) and zeolites (Novembre et al. 2011). In contrast to smectites, 2:1 clay minerals with substantial isomorphous substitution in the layers, kaolinites are 1:1 clay minerals with layers composed of one tetrahedral and one dioctahedral sheet (Brindley & Robinson 1946; Giese 1988; Murray et al. 1993) in which isomorphous substitutions of central atoms are rare (Evans & Guggenheim 1988). However, a small amount of octahedral iron in natural kaolinites was reported (e.g. Meads & Malden 1975; Mestdagh et al. 1980; Petit et al. 1999). Particle shape of kaolinite is regular and pseudo-hexagonal. One of substantial parameters affecting the utilization of kaolins is the "crystallinity" or degree of structural ordering of kaolinite (Plançon & Tchoubar 1977a,b; Plançon et al. 1988, 1989; Bookin et al. 1989). The level of kaolinite ordering is usually expressed by indices calculated from their X-ray diffraction patterns (Hinckley 1963; Plançon & Zacharie 1990; Aparicio et al. 2006).

The mean crystallite thickness of kaolinites, analysed by Bertaut-Warren-Averbach (BWA) technique, is also a significant parameter for description of the "crystallinity" of kaolinite minerals (Šucha et al. 1999). Another factor is the purity of the kaolin ore since raw kaolin may contain admixtures, typically quartz, micas or mixed-layer clay minerals, notably illite-smectite or Fe oxides and oxyhydroxides.

Acidification of the clays

Acid solutions (e.g. acid mine drainage water or acid rain) occurring in natural environment can modify properties of the clays and thus also their application (Dubíková et al. 2002; Egiebor & Oni 2007). Acidity is an important factor affecting the formation of clays (e.g. Sillitoe 2010; Kadir et al. 2011; Premović et al. 2012) and weathering pathways controlling processes of clay-mineral formation in acidic soils (Uzarowicz et al. 2011). Many studies were devoted to acid treatment of bentonites or smectites (Fijał et al. 1975; Číčel & Novák 1976; Stoch et al. 1977; Novák & Číčel 1978; Komadel et al. 1993, 1996; Tkáč et al. 1994; Breen et al. 1997; Madejová et al. 1998; Rožić et al. 2010, 2011; Sciascia et al. 2011), illites, micas or kaolinites (Bahranowski et al. 1993; Ganor et al. 1995; Kalinowski & Schweda 1996; Dubíková et al. 2002; Hradil et al. 2002; Jozefaciuk & Bowanko 2002; Pentrák et al. 2009, 2010; Nguetnkam et al. 2011; Valášková et al. 2011; Worasith et al. 2011). Acid attack on clay minerals causes very fast exchange of hydrated exchangeable cations mainly in smectites, typically Ca^{2+}, Na^{+}, Mg^{2+} and K^{+}, with H^{+} ions, which attack structural OH groups simultaneously with

depopulation of the octahedral Al, Fe and Mg from the structure. The presence of Mg and Fe (isomorphous substitutions for Al) in octahedral sheets leads to enhancement of the clay mineral dissolution due to higher negative layer charge density (Pentrák et al. 2012). The tetrahedra are rearranged from layered into three-dimensional adjustment. The protonated amorphous silica phase is the final reaction product (Tkáč et al. 1994; Madejová et al. 1998). The leaching effect of the acids on the clay minerals depends on temperature, time, type and concentration of used acid, clay/acid ratio and stirring of the reaction mixture. Solubility of the clay minerals in acids is also affected by type of clay minerals where chemical composition and swelling ability play important roles (Gates et al. 2002; Komadel 2003; Pentrák et al. 2010).

Origin of the sample

Kaolins occur in several different types of deposit in Slovakia. They were formed on weathering crusts of metamorphites and granitoids and rarely also on neovolcanites. The main period of kaolinization was from Badenian to Pontian (Kraus & Hano 1976; Kraus & Horváth 1978; Kraus 1989; Novotná et al. 1993; Madejová et al. 1997). Paleoclimatic development in this time span, in comparison to the older stage in the Paleogene, was less favourable and proceeded under lower average temperature and humidity (Kováč et al. 2006). Consequently, the process of chemical weathering showed lower intensity. Paleoenvironmental changes in the Central-Carpathian Paleogene Basin have been discussed recently in detail (Soták 2011). However, according to paleovegetation cover, a subtropical climate with gradual transition to warm temperate climatic conditions is still expected during the Miocene in the Central Parathethys (Kováčová et al. 2011).

The Vyšný Petrovec deposit is situated in a 10 km long and up to 1.5 km wide belt of kaolin sands with the greatest thickness of 80 m in the NW part of the Lučenská kotlina Depression (Hano 1973). It represents a redeposited kaolin crust of Horná Prievrana weathering type, situated just 3 km to the west-south west from the parent deposit (Fig. 1). Kaolin sands form an overburden of kaolinized sericitic-chloritic and sericitic-graphitic phyllites of Gemericum and it overlies sediments of the Poltár Formation (Kraus & Hano 1976).

Two distinct technological types of different mineralogical composition occur in both the primary kaolin of Horná Prievrana and the secondary sedimentary kaolin from Vyšný Petrovec (Kraus 1989). The first type, found only occasionally in the lower part of the deposit, consists of kaolinite, brammalite (Na-interlayer-deficient dioctahedral mica), illite and muscovite. The presence of brammalite indicates kaolinization on metarhyolites of Paleozoic age with a very high content of albite. The second type, a product of weathering of sericite-chlorite phyllites, is remarkably dominant. It comprises kaolinite, illite and muscovite, while brammalite and albite are absent. Kaolin from the Vyšný Petrovec deposit is considered to be the most promising source of domestic raw material for the Slovak ceramic and glass industry. Presence of both kaolin types, the weathering and sedimentary, confirms that the most extensive kaolin weathering of the Western Carpathians took place in SW part of the Veporicum and Gemericum (Kraus 1989). New potential application of kaolin from the Vyšný Petrovec deposit as metakaolin was reported recently. Metakaolin is a reactive aluminosilicate pozzolan obtained by thermal treatment of kaolin (at about 650 °C) and by grinding it to a high fineness. The use of metakaolin as a partial replacement for Portland cement clinker helps to obtain more eco-efficient cements (Krajčí et al. 2007; Janotka et al. 2010). The production of VP kaolin sand was about 20–30 kt per year. However, its production has been interrupted since 2009 (Baláž & Kúšik 2010) for economic reasons. The deposit is very heterogeneous, predomi-

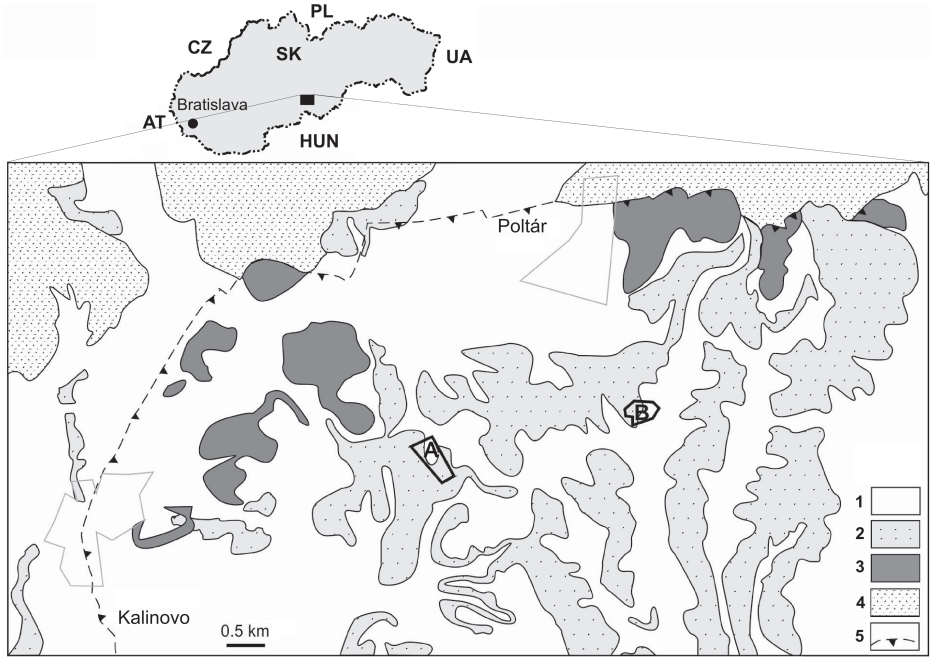

Fig. 1. Location of Vyšný Petrovec (A) and Horná Prievrana (B) deposits on the simplified geological map from Vass et al. 1992. **1** — Quaternary; **2** — Poltár Formation (Pont): variegated clays, sands and gravels; **3** — Gemericum: Dobšiná Group (Visean–Namurian A): phyllites with metasandstones, serpentinites; **4** — Veporicum: metamorphosed quartzy sandstones, sandstones, phyllites and intermediate to basic volcanoclastics; **5** — thrust lines.

nantly from the grain size point of view, and the production of raw material is connected with increased costs.

Kaolins KGa-1 (well-ordered) and KGa-2 (less-ordered) are the samples available from the Source Clays Repository of the Clay Minerals Society, used as reference materials over the years (Van Olphen & Fripiat 1979). An extensive amount of data is available in literature on these materials.

This study reports the stability of Vyšný Petrovec kaolin consisting of various minerals (kaolinites, micas, quartz, etc.) in HCl and the influence of components on its dissolution rate.

Materials and methods

Materials

The kaolin sand from Vyšný Petrovec (VP) (Slovakia) was studied. The sample was collected from a homogenized repository of mined kaolin sands that was situated directly in the deposit. To obtain the fine fraction of VP, 1 kg of the raw material was suspended in distilled water and treated with 1 mol·dm^{-3} $CaCl_2$ solution. After the sedimentation (using Stokes'law) the <45 μm fraction was collected, washed free of excess ions, air-dried at 60 °C and ground to pass a 0.2 mm sieve. Its chemical and mineralogical compositions are reported in Table 1 and Table 2, respectively.

Table 1: Chemical composition of <45 μm fraction of VP kaolin (in mass %) determined after drying at 105 °C.

Sample	SiO_2	Al_2O_3	Fe_2O_3	CaO	MgO	Na_2O	K_2O	TiO_2	H_2O	Total
VP	50.20	32.47	1.61	0.22	0.44	0.06	1.93	1.33	9.98	98.24

Methods

Acid treatments were performed at 95 °C for 4, 8, 12, 18 and 36 hours. 2.5 g of the <45 μm sample were mixed with 0.250 dm^3 of 6 mol·dm^{-3} HCl. This high concentration of acid, similarly as in Pentrák et al. (2009, 2010), was chosen to achieve faster structural changes of the clays than in the natural environment with weaker reaction conditions (Lintnerová et al. 1999; Dubíková et al. 2002). The suspensions were heated in 0.5 dm^3 glass flasks with laps under reflux. The mixtures were stirred every hour. The filtrate and wash supernatant solutions were analysed for Al, Fe and Si by atomic emission spectroscopy, yielding the amounts of the elements dissolved. Dissolution curves were constructed by plotting the undissolved fraction of the respective cation versus time (Komadel et al. 1996).

Powder X-ray diffraction. XRD profiles of pressed powder samples were collected on a BRUKER D8 Advance diffractometer equipped with CuKα ($\lambda\alpha_1$ = 1.54060 Å) radiation and a BRUKER LynxEye detector. The records were collected in the 2-theta range from 2.5° to 65°, using step of 0.01° 2Θ, and counting time of 3 s per step.

Quantitative analysis of the acid untreated sample was performed applying the RockJock program (Eberl 2003). The program fits the sum of stored XRD patterns of pure standard minerals (the calculated pattern) to the measured pattern by varying fraction of each mineral standard pattern, using the Solver function Microsoft Excel to minimize a degree of fit parameter between the calculated and measured pattern. Samples for analysis were prepared by adding 0.111 g ZnO (internal standard) to 1.000 g sample. The mixture was ground in a McCrone mill for 5 min with 4 ml of methanol then dried and sieved (Eberl 2003).

XRD profiles of *001* basal plane reflections of illite and kaolinite were selected for crystallite size determination of acid-untreated and treated samples. Selected peaks were fitted by pseudo-Voight function. This function is an analytical approximation of the Voigt function which in turn is the convolution product of a Gaussian and a Lorentzian function with the mixing factors h = 1 and h = 0, respectively. It provides refinement stability and the possibility of a crude physical interpretation of mixing factors h. The simple Scherrer equation, as integral breadth method was utilized for crystallite size determination by software Topas V2.0 (Bruker AXS, 2000). Values of reliability for profile fitting (Rwp) were always <4 %.

Infrared spectroscopy. Fourier transform infrared (FTIR) spectra in the middle IR (MIR) region (4000–400 cm^{-1}) were obtained using a Nicolet 6700 spectrometer and KBr pressed-disc technique (0.5 mg of sample and 200 mg of KBr). The discs were heated in a furnace overnight at 150 °C to minimize the water adsorbed on sample and KBr. For the near IR (NIR) region (12000–4000 cm^{-1}) neat samples were measured by a Smart Diffuse Reflectance (DRIFT) accessory from Thermo Scientific. 128 scans with resolution of 4 cm^{-1} were recorded for each sample. Spectra manipulations were performed using the Thermo Scientific OMNIC 8.0 software package.

Atomic emission spectroscopy (AES). The amounts of Al, Fe and Si leached from the samples upon the acid treatment were calculated from the data obtained on a Varian Vista-MPX optical emission spectrometer with inductively coupled plasma (ICP–OES) equipped with a 40 MHz air-cooled free running RF generation system, power (kW) 1.3 kW, plasma flow rate 1.5 dm^3·min^{-1} and the nebulizer flow rate 0.7 dm^3·min^{-1}.

Scanning electron microscopy (SEM). The morphology of the kaolin sand sample was displayed by an Electron microscope SEM LEO 1450VP with resolution of 3.5 nm, accelerating voltage of 30 kV, current probe of 20 pA and working distance of 8 mm.

Thermal analysis (TA). Differential thermal analysis (DTA) and thermogravimetric (TG) curves were obtained simultaneously using a TA Instruments SDT 2960 apparatus, sample mass of 25 mg, platinum crucible, heating rate of 10 °C·min^{-1} in air flow, temperature range 20–1100 °C and reference material Al_2O_3.

Results and discussion

Characterization of the acid-untreated <45 μm fraction of the VP kaolin sample

XRD analysis. XRD powder pattern analysis was used to determine the mineral composition of the acid-untreated sample.

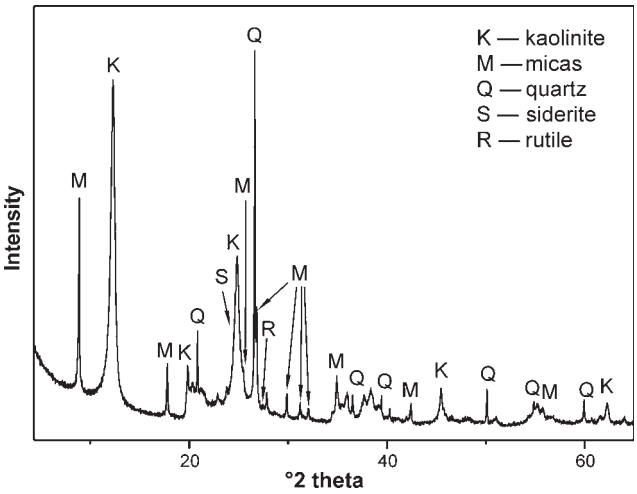

Fig. 2. XRD pattern of VP acid-untreated sample (CuKα radiation).

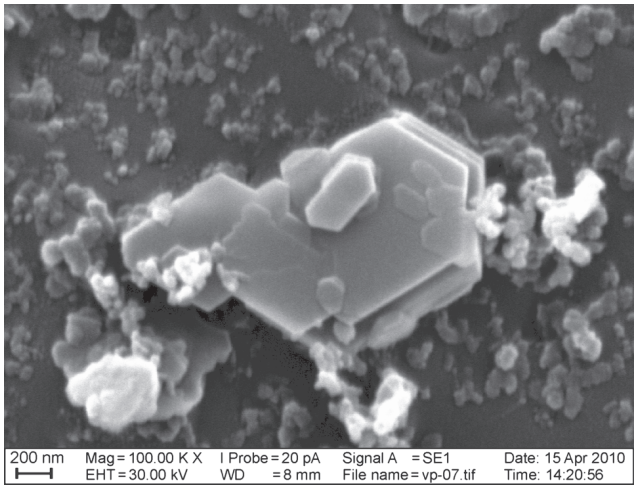

Fig. 3. SEM image of pseudohexagonal kaolinite particles in VP sample.

Table 2: Results of quantitative XRD analysis (RockJock) of < 45 μm fraction of VP kaolin.

	VP (mass %)
Kaolinite	60
Dioctahedral micas	32
Quartz	7
Siderite, Rutile	<2

Besides a kaolinite and mica type minerals, including a muscovite and an illite, the < 45 μm fraction of the VP sample also contains non-clay admixtures such as quartz (3.34 Å) and probably also a siderite and a rutile (Fig. 2). The mineral composition of the sample reveals that it belongs to the second type of kaolin occurring in the Vyšný Petrovec deposit. The results from quantitative RockJock analysis of the acid-untreated sample are presented in Table 2.

The structural ordering of kaolinite was determined by Hinckley index (HI) and Aparicio-Galán-Ferrel index (AGFI) described by Hinckley (1963) and Aparicio et al. (2006), respectively. While HI needs performance of decomposition of overlapped diffractions between 20° and 23° 2Θ to the distinguished peaks, AGFI requires only simple weighting peak intensity ratios of the *020*, *110*, and *111* diffractions. Moreover, the HI is influenced by the presence of quartz, feldspar, Fe-hydroxide gels, illite, smectite and halloysite, while the AGFI is less affected by the admixtures including X-ray amorphous phases (Aparicio et al. 1999; Galán et al. 2006). The calculated HI value of 0.63 for VP shows the presence of a medium defect kaolinite. The AGFI value of 1.3 also classifies this kaolinite to the medium defect kaolinite group (Aparicio et al. 2006).

Scanning electron microscopy. Figure 3 shows sharp edges of pseudohexagonal isolated particles of kaolinite with maximum dimensions of ~1 μm.

These kaolinite grains are small compared to those in well-ordered kaolinites KGa-1 and KGa-1b from Washington County, Georgia. Pruett & Webb (1993) estimated that 58 % of KGa-1b particles were smaller than 2 μm and 32 % were < 0.5 μm, whereas in KGa-1 it was about 47 and 21 %, re-

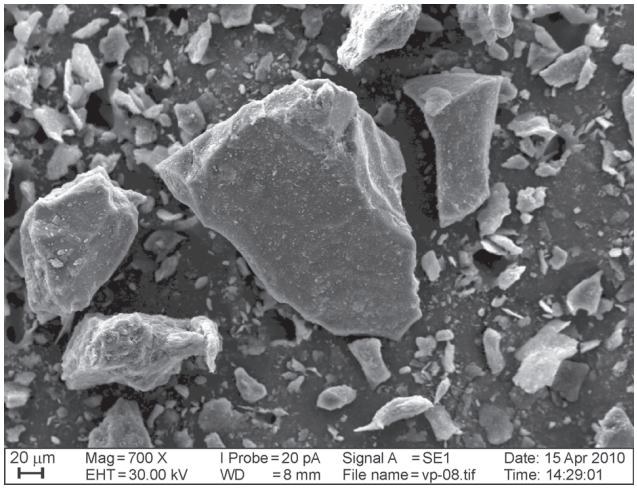

Fig. 4. SEM images of irregular quartz grains in VP sample.

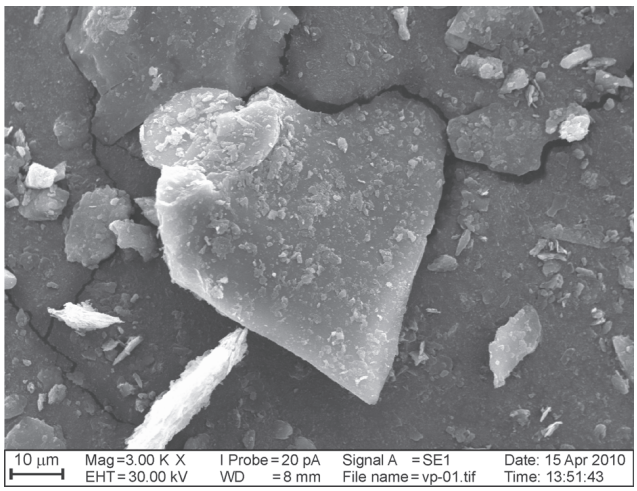

Fig. 5. SEM image of mica aggregates in VP sample.

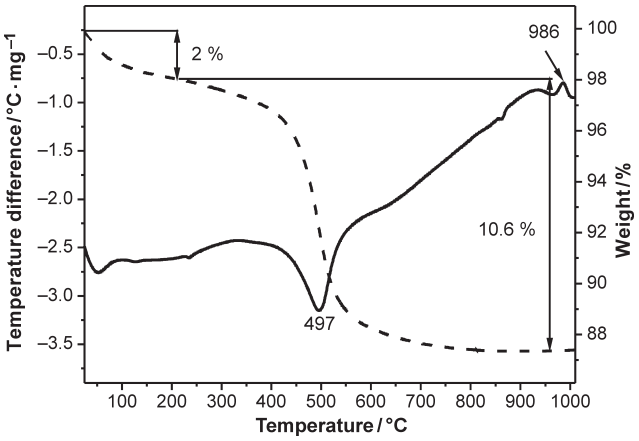

Fig. 6. TG and DTA experimental curves for VP sample.

spectively. Clearly identifiable irregular quartz grains had larger sizes of ~210 μm (Fig. 4).

Mica grains represented platy aggregates (Fig. 5). In comparison to quartz, the aggregates are of smaller average size (~70 μm).

Thermal analysis. Dehydration, dehydroxylation and recrystallization steps were found by thermal analysis of the acid-untreated sample. The TG curve shows two steps of mass loss from 20 up to 1000 °C (Fig. 6). The first step between room temperature and 200 °C represents 2 % mass reduction of water molecules from the surface. The second mass decrease of about 10 % occurring between 350 and 900 °C reflects dehydroxylation processes of kaolinite and mica type minerals. Due to very close dehydroxylation temperatures of these minerals (Bish & Duffy 1990) only one minimum at 497 °C related to metakaolinite formation was observed on the DTA curve (Siddique & Klaus 2009). The small exothermic peak at 986 °C corresponds to the formation of mullite (Brindley & Nakahira 1959; Slaughter & Keller 1959; Bulens & Delmon 1977). Guggenheim & Koster van Groos (2001) reported that the clay mineral standards KGa-1b (well-ordered) and KGa-2 (less-ordered) both containing ~96 % kaolinite (Chipera & Bish 2001) showed dehydroxylation maxima at 518 and 513 °C, respectively. Similarly, the exothermic maxima were found at 993 °C for KGa-1b and 984 °C for KGa-2, which is just above and below the 986 °C found for VP kaolin. These small differences can, at least partly, also be due to non-equal sample preparation and different instruments used. The admixtures present in VP kaolin (~40 mass %) could have affected its thermal stability.

IR spectroscopy. Further information on the chemical and structural composition of VP kaolin was obtained by IR spectroscopy in both MIR and NIR regions. Four resolved bands are observed in the OH stretching region (Fig. 7b). The band at 3697 cm^{-1} belongs to inner surface AlAlOH groups and vibration at 3621 cm^{-1} is attributed to inner AlAlOH groups. Two bands at 3670 and 3653 cm^{-1} are usually resolved only in the spectra of well-ordered kaolinites, disordered kaolinites show a single complex band near 3650 cm^{-1} (Farmer 1974; Madejová et al. 2002). Less clear resolution and lower intensity of the 3670 cm^{-1} band in the VP spectrum than in the spectrum of a well-ordered KGa-1b (Madejová & Komadel 2001) also indicates only medium-ordering of the kaolinite in the VP sample. The absence of the AlFeOH band near 3598 cm^{-1} implies that iron determined by chemical analysis of VP kaolin is not bound in the kaolinite's octahedral sheets (Petit et al. 1999). The absorption bands at 936 and 916 cm^{-1} correspond to bending vibration of inner-surface and inner OH groups, respectively. Three vibrations at 1105, 1034 and 1010 cm^{-1} represent Si-O stretching modes of tetrahedral sheets. Bending vibrations of Si-O-Al a Si-O-Si are located at 539 and 471 cm^{-1}, respectively (Fig. 7c). The OH and Si-O absorption bands of mica type mineral are overlapped by more intense bands of kaolinite. A characteristic doublet at 798 and 779 cm^{-1} confirms the presence of quartz.

The NIR spectrum of VP shows bands corresponding to the overtone $2\nu_{OH}$ and combination $(\nu+\delta)_{OH}$ modes of the fundamental vibrations of OH groups (Fig. 7a). The $2\nu_{OH}$ band near 7068 cm^{-1} belongs to vibrations of the inner OH groups, while the less intense band at 7171 cm^{-1} is due to $2\nu_{OH}$ overtone of inner-surface OH groups. The presence of water molecules in the sample is confirmed by the $(\nu+\delta)_{H_2O}$ band at 5225 cm^{-1}. This band is hardly recognized in the spectra of kaolins with high kaolinite content due to very low amount of water adsorbed on the particle edges (Pentrák et al. 2009). The combination bands of AlAlOH groups occur at 4622 and 4528 cm^{-1} (Fig. 7a).

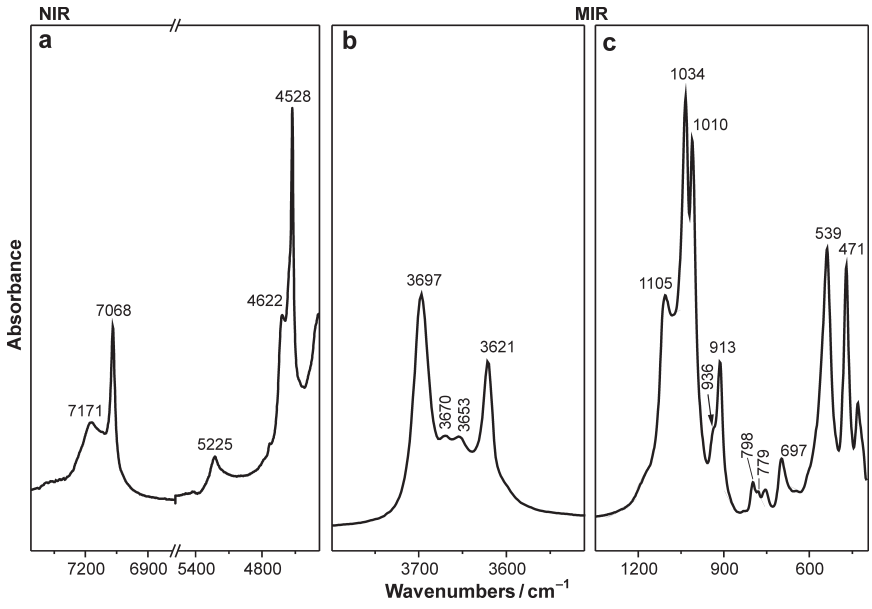

Fig. 7. MIR (b and c) and NIR (a) spectra of VP kaolin.

Acid dissolution

Structural changes of VP kaolin dissolved in HCl were monitored by XRD (Fig. 8). The intensities of the basal diffractions of present phyllosilicates decreased gradually proportionally to time of dissolution up to 12 hours (Fig. 8a–d). More profound changes were observed after longer dissolution times. Treatment for 18 hours caused almost total destruction of mica's structure, while the diffractions of kaolinite were still clearly visible (Fig. 8e).

Only some traces of kaolinite and mica type mineral can be detected after 36 hours of acid treatment. On the contrary, the resistance of quartz against high molar hydrochloric acid is well-documented mainly by absence of changes in the intensities of diffraction maxima at 26.6° 2Θ (3.34 Å, Fig. 8f).

A similar trend in crystallite size reduction was determined by analytical profile fitting of both, kaolinite and dioctahedral mica, *001* peaks and calculation based on the Scherrer equation (Table 3). The crystallite size of the longest treated dioctahedral micas was reduced to less than 15 % of those in the acid-untreated sample. Kaolinite was confirmed as the more stable phase; only less than 50 % reduction of crystallite size was determined in the most extensively dissolved material. The measured mean crystallite size of the untreated VP kaolinite is more than twice as large as the mean thickness of VP kaolinite and of other Slovak kaolinites determined by the BWA technique (Šucha et al. 1999). This discrepancy is caused by different approach to the calculation of the mean values. The integral breadth methods, applied in this study, use volume weighted column heights, in contrast to the BWA analysis using area weighted values (Klug & Alexander 1974; Drits et al. 1998).

Figure 9 shows dissolution of Al, Fe and Si from VP samples. The amount of individual elements remaining in the solid reaction product is plotted vs. time of dissolution. Because VP kaolin contains besides kaolinite also other clay and non-clay minerals more or less soluble in HCl, the resulting acid dissolution (AD) curves represent the sum of the individual elements dissolved from all minerals present. As expected, the release of Si atoms into the solution was minor due to formation of a protonated amorphous silica phase in the solid reaction product (Tkáč et al. 1994; Madejová et al. 2009; Pentrák et al. 2009).

The dissolution curve for Al shows that about 25 % of total Al is dissolved from VP kaolin after 4 hours; while the AD curve for Fe indicates about 50 % of total Fe released, implying that iron is bound in a phase more soluble in HCl than kaolinite. Higher extent of Fe release than that of Al was observed also after 12 hours of VP dissolution. The final solid reaction product contains 13 % and 12 % of total Al and Fe found in the starting material, respectively.

Pentrák et al. (2009) compared dissolution rates of two kaolins (GF, KGa-2)

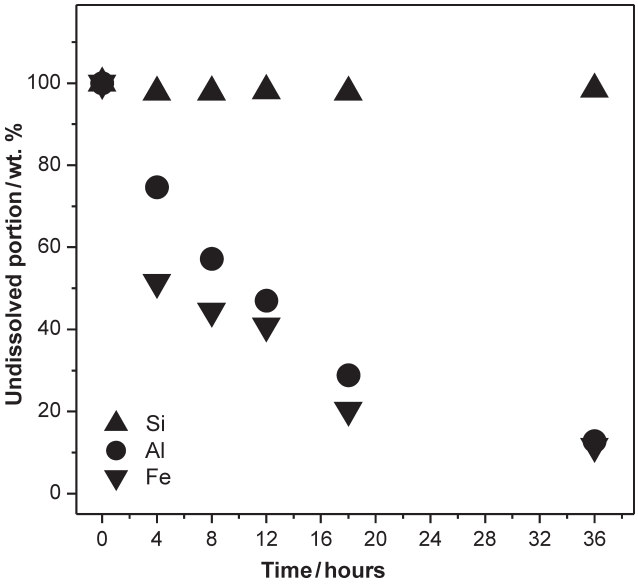

Fig. 9. Dissolution of Si, Al and Fe from VP kaolin in 6 mol·dm^{-3} HCl at 95 °C.

Table 3: Reduction of crystallite size of kaolinite and dioctahedral mica upon acid dissolution as determined by profile fitting followed by crystallite size calculation using Scherrer equation.

Time of acid treatment (hours)	Dioctahedral mica *001* Crystallite size (nm)		Kaolinite *001* Crystallite size (nm)	
0	80.7	± 9.3	19.0	± 0.4
4	61.7	± 3.9	17.7	± 0.2
8	64.9	± 4.5	17.1	± 0.3
12	58.5	± 4.2	16.3	± 0.4
18	27.1	± 3.0	15.2	± 0.4
36	12.1	± 1.2	10.3	± 0.5

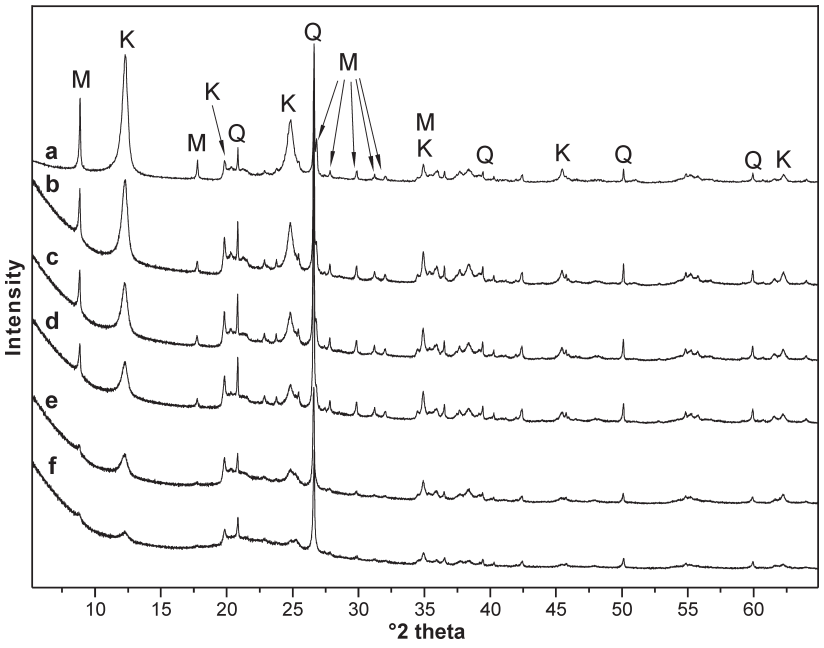

Fig. 8. XRD patterns of untreated (a) VP kaolin and treated in 6 mol·dm^{-3} HCl at 95 °C for 4 (b), 8 (c), 12 (d), 18 (e) and 36 h (f).

with similar chemical composition and different structural ordering ($AGFI_{KGa-2}$ = 0.8; $AGFI_{GF}$ = 1.6) in 6 mol·dm^{-3} HCl at 95 °C. Although Fe occurred in both samples, the IR spectra confirmed the presence of Fe in the octahedral sheets only for well-ordered Golden Field (GF) kaolinite. About 50 % of total Al and Fe remained undissolved after 36 hours of treatment of the well-ordered GF, in contrast to less-ordered KGa-2, for which only 16 % of Al and Fe resisted the dissolution process. It follows that a higher level of structural ordering of GF kaolinite increases its stability against the acid attack. Hradil et al. (2002) also described the same results. As both the HI and AGFI indices confirm, the mineral in VP kaolin is a middle-ordered kaolinite. The AD curves of VP kaolin, however, show an even larger extent of decomposition after 36 hours in HCl than less-ordered KGa-2, dissolved under the same conditions (Pentrák et al. 2009). The presence of more soluble minerals (e.g. mica type minerals) than kaolinite accelerates the dissolution of VP kaolin.

Useful information on the extent of VP kaolin dissolution provides IR spectroscopy in both MIR (Fig. 10) and NIR (Fig. 11) regions. The changes observed in the Si-O stretching and bending regions reflect the transformation of the layered structure into a three-dimensional framework. Intensities of the Si-O stretching bands at 1034 and 1010 cm^{-1} decrease upon acid treatment and after 36 hours of dissolution they are hardly distinguishable. Simultaneous appearance of the bands at 1105 and 800 cm^{-1} indicates formation of an amorphous SiO_2 phase in the solid reaction product (Fig. 10).

Gradual release of octahedral atoms from the clay minerals present in VP kaolin is reflected in a progressive decrease of the intensities of the OH stretching bands in the 4000–3000 cm^{-1} region and the AlAlOH bending bands at 936 and 913 cm^{-1}.

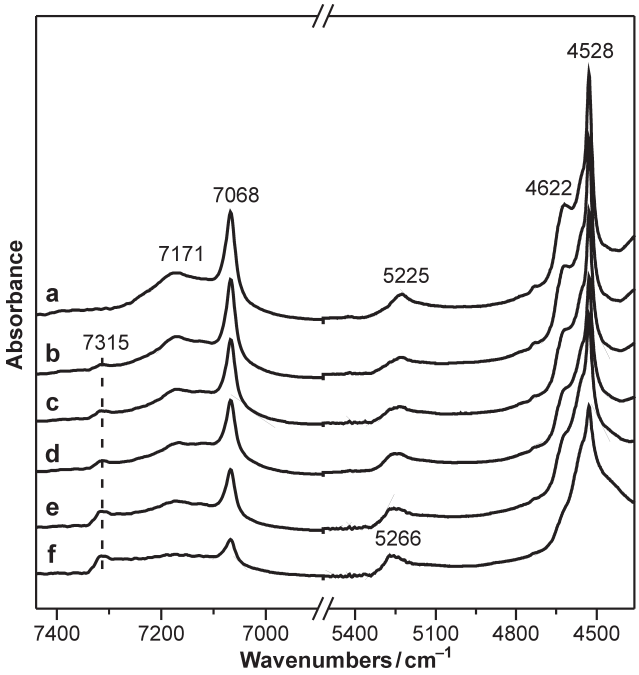

Fig. 11. NIR spectra of untreated (a) VP kaolin and treated in 6 mol·dm^{-3} HCl at 95 °C for 4 h (b), 8 h (c), 12 h (d), 18 (e) and 36 h (f).

Liberation of Al atoms into HCl solution is also confirmed by decreasing intensity of the Al-O-Si band at 539 cm^{-1} (Fig. 10d). Although the absorption bands of amorphous silica at 1100, 800 and 470 cm^{-1} dominate in the MIR spectrum of VP after 36 hours of dissolution in HCl, clearly resolved bands of kaolinite prove the considerable stability of this clay mineral. This is in agreement with the Al AD curve indicating that about 13 % of total Al remains in the solid reaction product (Fig. 10f).

Structural destruction of VP kaolin in HCl can also be seen in the NIR spectra (Fig. 11). Significant reduction in the intensities of the structural OH overtones at 7171 and 7068 cm^{-1} and OH combination modes near 4622 and 4528 cm^{-1} starts after 8 hours of acid treatment. In spite of substantial decrease in the amount of AlAlOH groups with prolonged time of dissolution, complex OH overtone and combination bands can be observed even in the NIR spectrum of VP kaolin treated for 36 hours (Fig. 11f).

The appearance of the $2\nu_{Si-OH}$ overtone at 7315 cm^{-1} after 4 hours of acid treatment confirms partial protonization of Si-O bonds (Fig. 11b). Enhancing intensity with prolonged time of treatment indicates an increasing amount of SiOH groups. Decomposition of VP kaolin in HCl also influences the adsorption of water on clay mineral surfaces. The combination band of water molecules $(\nu + \delta)_{H_2O}$ is seen near 5225 cm^{-1} in the NIR spectrum of untreated VP kaolin. Upon acid treatment, the position of the band is shifted to ~5266 cm^{-1}, namely to the same position as observed in the NIR spectra of extensively

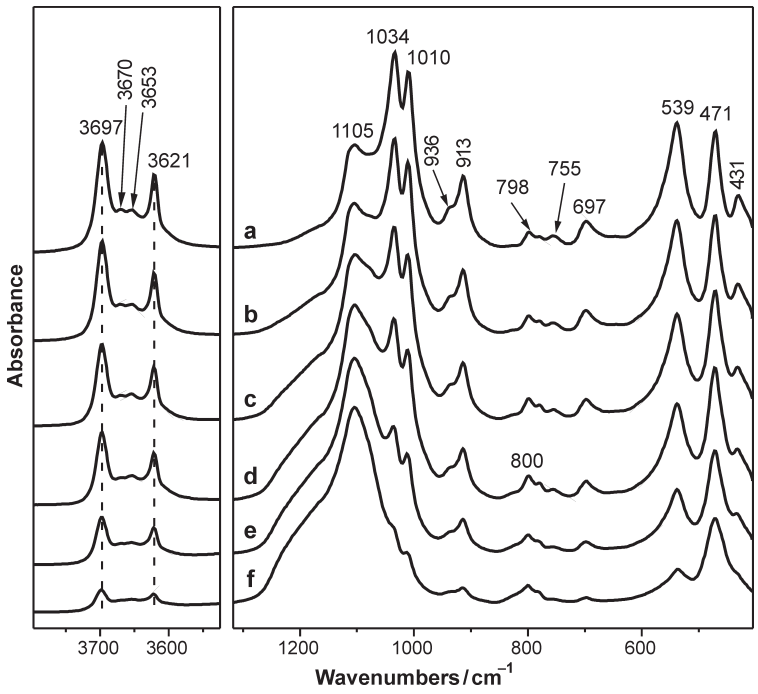

Fig. 10. MIR spectra of untreated (a) VP kaolin and treated in 6 mol·dm^{-3} HCl at 95 °C for 4 h (b), 8 h (c), 12 h (d), 18 (e) and 36 h (f).

acid-decomposed smectites and illites (Madejová et al. 2009). The shift of the water band reflects different strength of H-bonds between water molecules and acid-untreated clay minerals and between H_2O and amorphous silica, created upon clay minerals dissolution. Moreover, the final position of the $(\nu + \delta)_{H_2O}$ band confirms, like all bands observed in the MIR and NIR spectra of the 36 hours treated VP, that dissolution of kaolinite results in the same reaction product as that of other clay minerals.

Conclusions

The less than 45 μm fraction of kaolin sand from Vyšný Petrovec deposit in Slovakia contains about 60 % of medium-ordered kaolinite, 32 % of dioctahedral mica type minerals and about 9 % of non-clay minerals, mainly quartz. However, the stability of this kaolin in strongly acidic environment is lower than that of less-ordered KGa-2 kaolinite. Chemical analysis, XRD and IR spectroscopy confirm almost complete decomposition of the clay minerals present in the acid-untreated VP kaolin upon a 36 hours treatment in 6 $mol \cdot dm^{-3}$ HCl at 95 °C. The small-grain size of the middle-ordered kaolinite and the presence of accessory minerals (illite, siderite), more soluble than kaolinite, are responsible for the lower stability of Vyšný Petrovec kaolin in HCl than pure kaolinite samples under the same conditions.

Acknowledgments: The financial support of the Slovak Grant Agency VEGA (Grant 2/0183/09) and Slovak Research and Development Agency (Grant APVV-VVCE-0033-07) are highly appreciated. We express gratitude to Professor V.N. Sokolov (Lomonosov Moscow State University) for his excellent SEM measurements and Professor I. Kraus (Comenius University, Bratislava) for his willingness to share his knowledge on kaolins.

References

Aparicio P. & Galán E. 1999: Mineralogical interference on kaolinite crystallinity index measurements. *Clays and Clay Miner.* 47, 12–27.

Aparicio P., Galán E. & Ferrell R.E. 2006: A new kaolinite order index based on XRD profile fitting. *Clay Miner.* 41, 811–817.

Bahranowski K., Serwicka E.M., Stoch L. & Strychalski P. 1993: On the possibility of removal of non-structural iron from kaolinite-group minerals. *Clay Miner.* 28, 379–391.

Baláž P. & Kúšik D. (Eds.) 2010: Slovak Minerals Yearbook. Statistical data to 2009. *State Geological Institute of Dionýz Štúr*, 1–158.

Bish D.L. & Duffy C.J. 1990: Thermogravimetric analysis of minerals. In: Stucki J.W. & Bish D.L. (Eds.): Thermal analysis in clay science. *CMS Workshop Lectures. Clay Minerals Society, Boulder*, Colorado, USA, 124–129.

Bookin A.S., Drits V.A., Plançon A. & Tchoubar C. 1989: Stacking faults in kaolin-group minerals in the light of real structural features. *Clays and Clay Miner.* 37, 297–307.

Breen C., Zahoor F.D., Madejová J. & Komadel P. 1997: Characterization and catalytic activity of acid-treated, size-fractionated smectites. *J. Physical Chemistry B* 101, 5324–5331.

Brindley G.W. & Nakahira M. 1959: The kaolinite-mullite reactions series. I. A survey of outstanding problems. II. Metakaolin. III. The high temperature phases. *J. Amer. Ceramic Soc.* 42, 311–324.

Bruker AXS 2000, TOPAS V2.0: General profile and structure analysis software for powder diffraction data. *User Manual*, Bruker AXS, Karlsruhe, Germany.

Bulens M. & Delmon B. 1977: The exothermic reaction of metakaolinite in the presence of mineralizers. Influence of crystallinity. *Clays and Clay Miner.* 25, 271–277.

Chipera S.J. & Bish D.L. 2001: Baseline studies of the Clay Minerals Society Source Clays: Powder X-ray diffraction analyses. *Clays and Clay Miner.* 49, 398–409.

Číčel B. & Novák I. 1976: Dissolution of smectites in hydrochloric acid. I. Half-time of dissolution as a measure of reaction rate. *7-th Conference on Clay Mineralogy and Petrology*, Karlovy Vary.

Drits V.A., Eberl D.D. & Środoń J. 1998: XRD measurement of mean thickness, thickness distribution and strain for illite and illite-smectite crystallites by the Bertaut-Warren-Averbach technique. *Clays and Clay Miner.* 46, 38–50.

Dubíková M., Cambier P., Šucha V. & Čaplovičová M. 2002: Experimental soil acidification. *App. Geochem.* 17, 245–257.

Eberl D.D. 2003: User's guide to RockJock — a program for determining quantitative mineralogy from powder X-ray diffraction data. *U.S. Geol. Surv., Open-File Report,* 3–78.

Egiebor N.O. & Oni B. 2007: Acid rock drainage formation and treatment: a review. *Asia-Pacific J. Chem. Engineering* 2, 47–62.

Evans B.W. & Guggenheim S. 1988: Talc, pyrophyllite and related minerals. In: Bailey S.W. (Ed.): Hydrous phyllosilicates (exclusive of micas). *Rev. in Mineralogy*, 19, *Mineral. Soc. Amer.*, Washington, D.C., 225–294.

Farmer V.C. 1974: Layer silicates. In: Farmer V.C. (Ed.): Infrared spectra of minerals. Monograph. *Mineral. Soc., London* 4, 331–363.

Fijał J., Kłapyta Z., Ziętkiewicz J. & Żyła M. 1975: On the mechanism of the montmorillonite acid activation. I. Degradation of Ca-montmorillonite structure. *Mineral. Pol.* 6, 29–43.

Galán E., Aparicio P., La Iglesia A. & González I. 2006: The effect of pressure on order/disorder in kaolinite under wet and dry conditions. *Clays and Clay Miner.* 54, 232–241.

Ganor J., Mogollon J.L. & Lasaga A.C. 1995: The effect of pH on kaolinite dissolution rates and on activation energy. *Geochim. Cosmochim. Acta* 59, 1037–1052.

Giese R.F. 1988: Kaolin minerals: Structures and stabilities. In: Bailey S.W. (Ed.): Hydrous phyllosilicates (exclusive of micas). *Rev. in Mineralogy*, 19, *Mineral. Soc. Amer.*, Washington, D.C., 29–66.

Guggenheim S. & Koster van Groos A.F. 2001: Baseline studies of the Clay Minerals Society Source Clays: Thermal analysis. *Clays and Clay Miner.* 49, 433–443.

Hano V. 1973: Vyšný Petrovec, preliminary exploration — kaolin sands. *Report, Geofond*, Bratislava, 1–74 (in Slovak).

Harvey C.C. & Lagaly G. 2006: Conventional applications. In: Bergaya F., Theng B.K.G. & Lagaly G. (Eds.): Handbook of clay science. Developments in clay science. Vol. 1. *Elsevier Ltd.*, The Netherlands, 501–540.

He M.C., Zhao J., Fang Z.J. & Zhang P. 2011: First-principles study of isomorphic ('dual-defect'). *Clays and Clay Miner.* 59, 501–506.

Hinckley D.N. 1963: Variability in "crystallinity" values among the kaolin deposits of the coastal plain of Georgia and South Carolina. In: Swineford A. (Ed.): *Clays and Clay Miner.*, *Proc. 11th Natl. Conf.*, Ottawa, Ontario, 1962. Pergamon, New York, 229–235.

Hradil D., Hostomský J. & Soukupová J. 2002: Aluminium release

rates from acidified clay structures: comparative kinetic study. *Geol. Carphathica* 53, 2, 117–121.

Janotka I., Puertas F., Palacios M., Kuliffayová M. & Varga C.I. 2010: Metakaolin sand-blended-cement pastes: Rheology, hydration process and mechanical properties. *Construction and Building Materials* 24, 791–802.

Jozefaciuk G. & Bowanko G. 2002: Effect of acid and alkali treatments on surface areas and adsorption energies of selected minerals. *Clays and Clay Miner.* 50, 771–783.

Kadir S., Erman H. & Erkoyun H. 2011: Mineralogical and geochemical characteristics and genesis of hydrothermal kaolinite deposits within neogene volcanites, Kütahya (Western Anatolia), Turkey. *Clays and Clay Miner.* 59, 250–276.

Kalinowski B.E. & Schweda P. 1996: Kinetics of muscovite, phlogopite and biotite dissolution and alteration at pH 1–4, room temperature. *Geochim. Cosmochim. Acta* 60, 367–385.

Klug H.P. & Alexander L.E. 1974: X-ray diffraction procedures for polycrystalline and amorphous materials. 2nd edition. *Wiley*, New York, USA, 1–992.

Komadel P., Stucki J.W. & Čičel B. 1993: Readily HCl-soluble iron in the fine fractions of some Czech bentonites. *Geol. Carpathica — Clays* 44, 11–16.

Komadel P., Madejová J., Janek M., Gates W.P., Kirkpatrick R.J. & Stucki J.W. 1996: Dissolution of hectorite in inorganic acids. *Clays and Clay Miner.* 44, 228–236.

Komadel P. 2003: Chemically modified smectites. *Clay Miner.* 38, 127–138.

Kováč M., Baráth I., Fordinál K., Grigorovich A.S., Halásová E., Hudáčková N., Joniak P., Sabol M., Slamková M., Sliva Ľ. & Vojtko R. 2006: Late Miocene to Early Pliocene sedimentary environments and climatic changes in the Alpine-Carpathian-Pannonian junction area: A case study from the Danube Basin northern margin (Slovakia). *Palaeogeogr. Palaeoclimatol. Palaeoecol.* 238, 32–52.

Kováčová M., Doláková N. & Kováč M. 2011: Miocene vegetation pattern and climate change in the northwestern Central Paratethys domain (Czech and Slovak Republic). *Geol. Carphathica* 62, 3, 251–266.

Krajči Ľ., Janotka I., Kraus I. & Jamnický P. 2007: Burnt kaolin sand as pozzolanic material for cement hydration. *Ceramics-Silikáty* 51, 217–224.

Kraus I. 1989: Kaolins and kaolinite clays of the Western Carpathians. Western Carpathians, mineralogy petrography geochemistry metalogensis series. *Geological Institute of Dionýz Štúr,* Bratislava 13, 1–287.

Kraus I. & Hano V. 1976: Genetic classification and age of kaolinite group minerals from the Western Carpathians deposits. *Miner. Slovaca* 8, 431–436 (in Slovak).

Kraus I. & Horváth I. 1978: Mineralogy and age of Slovakian kaolins. *Schrift. Geol. Wissenschaft.* 11, 125–136.

Lagaly G. 1999: Introduction: from clay mineral–polymer interaction to clay mineral-polymer nanocomposites. *Applied Clay Sci.* 15, 1–9.

Lintnerová O., Šucha V. & Streško V. 1999: Mineralogy and geochemistry of acid mine Fe-precipitates from the main Slovak mining regions. *Geol. Carpathica* 50, 395–404.

Ma M. 2011: The dispersive effect of sodium silicate on kaolinite particles in process water: Implications for iron-ore processing. *Clays and Clay Miner.* 59, 233–239.

Madejová J. & Komadel P. 2001: Baseline studies of The Clay Minerals Society Source Clays: Infrared methods. *Clays and Clay Miner.* 49, 410–432.

Madejová J., Kraus I., Tunega D. & Šamajová E. 1997: Fourier transform infrared spectroscopic characterisation of kaolinite group minerals from the main Slovak deposits. *Geol. Carpathica — Clays* 6, 3–10.

Madejová J., Bujdák J., Janek M. & Komadel P. 1998: Comparative FT-IR study of structural modifications during acid treatment of dioctahedral smectites and hectorite. *Spectrochim. Acta, Part A* 54, 1397–1406.

Madejová J., Kečkéš J., Pálková H. & Komadel P. 2002: Identification of components in smectite/kaolinite mixtures. *Clay Miner.* 37, 377–388.

Madejová J., Pentrák M., Pálková H. & Komadel P. 2009: Near-infrared spectroscopy: A powerful tool in studies of acid-treated clay minerals. *Vibrational Spectroscopy* 49, 211–218.

Matusik J., Gaweł A., Bielańska E., Osuch W. & Bahranowski K. 2009: The effect of structural order on nanotubes derived from kaolin-group minerals. *Clays and Clay Miner.* 57, 452–464.

Matusik J., Gaweł A., Bielańska E. & Bahranowski K. 2011: Surface area and porosity of nanotubes obtained from kaolin minerals of different structural order. *Clays and Clay Miner.* 59, 116–135.

Meads R.E. & Malden P.S. 1975: Electron-spin resonance in natural kaolinites containing Fe^{3+} and other transition metal ions. *Clay Miner.* 10, 313–345.

Mestdagh M.M., Vielvoye L. & Herbillon A.J. 1980: Iron in kaolinites. II. The relationship between kaolinite crystallinity and iron content. *Clay Miner.* 15, 1–13.

Moussi B., Medhioub M., Hatira N., Yans J., Hajjaji W., Rocha F., Labrincha J.A. & Jamoussi F. 2011: Identification and use of white clayey deposits from the area of Tamra (northern Tunisia) as ceramic raw materials. *Clay Miner.* 46, 165–175.

Murray H.H., Bundy W.M. & Harvey C.C. 1993: Kaolin genesis and utilization. Spec. Publ. No. 1. *Clay Miner. Soc*., Boulder, CO, 1–341.

Murray H.H. 2007: Applied clay mineralogy. Occurrences, processing and application of kaolins, bentonites, palygorskite-sepiolite, and common clays. *Elsevier, Developments in Clay Sci.* 2, 1–180.

Nguetnkam J.P., Kamga R., Villiéras F., Ekodeck G.E., Razafitianamaharavo A. & Yvon J. 2011: Alteration of cameroonian clays under acid treatment. Comparison with industrial adsorbents. *Applied Clay Sci.* 52, 122–132.

Novák I. & Čičel B. 1978: Dissolution of smectites in hydrochloric acid: II. Dissolution rate as a function of crystallochemical composition. *Clays and Clay Miner.* 26, 341–344.

Novembre D., Di Sabatino B., Gimeno D. & Pace C. 2011: Synthesis and characterization of Na-X, Na-A and Na-P zeolites and hydroxysodalite from metakaolinite. *Clay Miner.* 46, 339–354.

Novotná M., Kraus I. & Horváth I. 1993: Expression of kaolinite ordering in selected kaolin deposits. *Miner. Slovaca* 25, 55–59 (in Slovak).

Pentrák M., Madejová J. & Komadel P. 2009: Acid and alkali treatment of kaolins. *Clay Miner.* 44, 511–523.

Pentrák M., Madejová J. & Komadel P. 2010: Effect of chemical composition and swelling on acid dissolution of 2:1 clay minerals. *Philosophical Mag.* 90, 2387–2397.

Pentrák M., Czímerová A., Madejová J. & Komadel P. 2012: Changes in layer charge of clay minerals upon acid treatment as obtained from their interactions with methylene blue. *Applied Clay Sci.* 55, 100–107.

Petit S., Madejová J., Decarreau A. & Martin F. 1999: Characterization of octahedral substitutions in kaolinites using near infrared spectroscopy. *Clays and Clay Miner.* 47, 103–108.

Plançon A. & Tchoubar C. 1977a: Determination of structural defects in phyllosilicates by X-ray powder difraction. I. Principle of calculation of the diffraction phenomenon. *Clays and Clay Miner.* 25, 430–435.

Plançon A. & Tchoubar C. 1977b: Determination of structural defects in phyllosilicates by X-ray powder difraction. II. Nature and proportion of defects in natural kaolinites. *Clays and Clay Miner.* 25, 436–450.

Plançon A., Giese R.F. & Snyder R. 1988: The Hinckley index for kaolinites. *Clay Miner.* 23, 249–260.

Plançon A., Giese R.F., Snyder R., Drits V.A. & Bookin A.S. 1989: Stacking faults in the kaolin-group minerals: defect structures of kaolinite. *Clays and Clay Miner.* 37, 203–210.

Plançon A. & Zacharie C. 1990: An expert system for the structural characterization of kaolinite. *Clay Miner.* 25, 249–260.

Premović P.I., Ciesielczuk J., Bzovska G. & Đorđević M.G. 2012: Geochemistry and electron spin resonance of hydrothermal dickite (Nowa Ruda, Lower Silesia, Poland): vanadium and chromium. *Geol. Carphathica* 63, 3, 241–252.

Pruett R.J. & Webb H.L. 1993: Sampling and analysis of KGa-1B well-crystallized kaolin source clay. *Clays and Clay Miner.* 41, 514–519.

Rožić L., Novaković T. & Petrović S. 2010: Modeling and optimization process parameters of acid activation of bentonite by response surface methodology. *Applied Clay Sci.* 48, 154–158.

Rožić L., Grbić B., Radić N., Petrović S., Novaković T., Vuković Z. & Nedić Z. 2011: Mesoporous 12-tungstophosphoric acid/activated bentonite catalysts for oxidation of 2-propanol. *Applied Clay Sci.* 53, 151–156.

Sciascia L., Turco Liveri M.L. & Merli M. 2011: Kinetic and equilibrium studies for the adsorption of acid nucleic bases onto K10 montmorillonite. *Applied Clay Sci.* 53, 657–668.

Siddique R. & Klaus J. 2009: Influence of metakaolin on the properties of mortar and concrete: A review. *Applied Clay Sci.* 43, 392–400.

Sillitoe R.H. 2010: Porphyry copper systems. *Econ. Geol.* 105, 3–41.

Slaughter M. & Keller W.D. 1959: High temperature phases from impure Kaolin clays. *Bull. Amer. Ceramic Soc.* 38, 703–707.

Soták J. 2011: Paleoenvironmental changes across the Eocene-Oligocene boundary: insights from the Central-Carpathian Paleogene Basin. *Geol. Carphathica* 61, 5, 393–418.

Stoch L., Bahranowski K., Budek L. & Fijał J. 1977: Bleaching properties of non-bentonitic clay materials and their modification. I. Acid activation of the miocene clays from Machów. *Miner. Pol.* 8, 31–51.

Šucha V., Kraus I., Šamajová E. & Puškelová Ľ. 1999: Crystallite size distribution of kaolin minerals. *Periodico di Mineralogia* 68, 81–92.

Tkáč I., Komadel P. & Müller D. 1994: Acid-treated montmorillonites — a study by ^{29}Si and ^{27}Al MAS NMR. *Clay Miner.* 29, 11–19.

Uzarowicz Ł., Skiba S., Skiba M. & Michalik M. 2011: Clay-mineral formation in soils developed in the weathering zone of pyrite-bearing schists: A case study from the abandoned pyrite mine in Wieściszowice, Lower Silesia, SW Poland. *Clays and Clay Miner.* 59, 581–594.

Valášková M., Barabaszová K., Hundáková M., Ritz M. & Plevová E. 2011: Effect of brief milling and acid treatment on two ordered and disordered kaolinite structures. *Applied Clay Sci.* 54, 70–76.

Van Olphen H. & Fripiat J.J. 1979: Data handbook for clay minerals and other non-metallic materials. *Pergamon Press*, 1–346.

Vass D., Elečko M., Bezák V., Bodnár J., Konečný V., Lexa J., Molák B., Straka P., Stankovič J., Stolár M., Škvarka L., Vozár J. & Vozárová A. 1992: Geological map of the Lučenská kotlina depression and Cerová vrchovina upland, 1:50,000. *Geol. Surv. of Slovak Republic*, Bratislava.

Worasith N., Goodman B.A., Neampan J., Jeyachoke N. & Thiravetyan P. 2011: Characterization of modified kaolin from the Ranong deposit Thailand by XRD, XRF, SEM, FTIR and EPR techniques. *Clay Miner.* 46, 539–559.

Yanik G. 2011: Mineralogical, crystallographic and technological characteristics of Yaylayolu kaolin (Kütahya, Turkey). *Clay Miner.* 46, 397–410.